NUMERICAL INVESTIGATION OF AN ADAPTIVE VIBRATION ABSORBER USING SHAPE MEMORY ALLOYS

Marcelo A. Savi, savi@mecanica.ufrj.br
Aline S. de Paula, aline@lavi.coppe.ufrj.br
Universidade Federal do Rio de Janeiro
COPPE – Department of Mechanical Engineering
21.945.970 – Rio de Janeiro – RJ – Brazil, Cx. Postal 68.503

Dimitris C. Lagoudas, lagoudas@aeromail.tamu.edu
Texas A&M University
Department of Aerospace Engineering
77843-3409 – College Station – Texas, USA

Abstract. *The tuned vibration absorber (TVA) is a well-established vibration passive control device for achieving vibration reduction of a primary system subjected to external excitation. The TVA consists of a secondary oscillatory system that once attached to a primary system is capable of absorbing vibration energy from the primary system. This contribution deals with the nonlinear dynamics of an adaptive tuned vibration absorber (ATVA) with a shape memory alloy (SMA) element. Initially, a single-degree of freedom oscillator with an SMA element is analyzed showing the general characteristics of its dynamical response. Then, the analysis of an SMA-ATVA is carried out starting, first by considering small amplitude vibrations in such a way that the SMA element does not undergo a stress-induced phase transformation. Under this assumption, the SMA influence is only caused by stiffness changes corresponding to temperature-induced phase transformation. Afterwards, the influence of the hysteretic behavior due to stress-induced phase transformation is considered. A proper constitutive description is employed in order to capture general thermomechanical aspects of the SMAs. The hysteretic behavior introduces complex characteristics to the system dynamics but also changes the absorber response allowing vibration reduction in different frequency ranges. Numerical simulations establish comparisons of the SMA-ATVA results with those obtained from the classical TVA.*

Keywords: *Control, vibration absorber, shape memory alloys, nonlinear dynamics, hysteresis, smart materials.*

1. INTRODUCTION

Vibration control is an essential task in engineering being related to different applications. The main goal is vibration reduction by employing either active or passive procedures. The tuned vibration absorber (TVA) is a well-established vibration passive control device for achieving reduction in the vibration of a primary system subject to external excitation (Inman, 1989; Meirovitch, 1986). The TVA consists of a secondary oscillatory system that once attached to the primary system is capable of absorbing vibration energy from the primary system. By tuning the natural frequency of the TVA to a chosen excitation frequency, one produces an attenuation of the primary system vibration amplitude for this specific forcing frequency. An alternative for systems where the forcing frequency varies or has a kind of uncertainty is the conception of an adaptive tuned vibration absorber (ATVA). This device is an adaptive–passive vibration control similar to a TVA but with adaptive elements that can be used to change the tuned condition (Ibrahim, 2008; Brennan, 2006).

The remarkable properties of shape memory alloys (SMAs) are attracting technological interest in several science and engineering fields and numerous applications have been developed exploiting singular characteristics of these alloys (Lagoudas, 2008; Paiva & Savi, 2006; Machado & Savi, 2003). In terms of applied dynamics, SMAs are being used in order to explore adaptive dissipation associated with hysteresis loop and the mechanical property changes due to phase transformation (Savi *et al.*, 2008; van Humbeeck, 2003). Moreover, the dynamical response of systems with SMA actuators presents a unique dynamical behavior due to their intrinsic nonlinear characteristic, presenting periodic, quasi-periodic and chaotic responses (Savi & Pacheco, 2002; Machado *et al.*, 2003, 2008; Bernardini & Rega, 2005; Savi *et al.*, 2008). Recently, SMA constraints have been used for vibration reduction since it is expected that the high dissipation capacity of SMA changes the system response producing less complex behaviors (Sitnikova *et al.*, 2008a,b; Santos & Savi, 2007).

In this regard, SMAs have been used in a number of approaches to passive structural vibration control (Machado *et al.*, 2009; Lagoudas *et al.*, 2004; Salichs *et al.*, 2001; Saadat *et al.*, 2002). SMA characteristics motivate the concept of an adaptive tuned vibration absorber (ATVA) that is able to change its stiffness depending on the SMA element's temperature (Elahinia *et al.*, 2005). This property allows one to attenuate primary system vibration amplitudes not only for one specific forcing frequency, as occurs with the TVA, but for a range of frequencies.

Williams *et al.* (2002) presented an adaptive-passive vibration controller using SMA elements in an ATVA. The device is manually tuned in order to achieve attenuation of vibration of the primary system across a range of frequencies. Williams *et al.* (2005) showed a continuously tuned SMA-ATVA as a novel adaptive–passive vibration

control device. The same idea was used in Rustighi *et al.* (2005a) that treated an SMA-ATVA made from a beam-like structure supported in its center. Numerical and experimental tests were performed showing that a change in the stiffness of the ATVA can be obtained by a temperature variation, which changes the Young's modulus, resulting in a variation of the tuning frequency. Rustighi *et al.* (2005b) presented control algorithms for real-time adaptation of this SMA-ATVA device both theoretically and experimentally. In general, the literature discusses the effect of property change due to the temperature-induced phase transformation in SMA-ATVA devices, but does not treat the influence of the hysteretic behavior due to stress-induced phase transformation.

This article deals with the nonlinear dynamics of an SMA-ATVA. Initially, a single-degree of freedom oscillator with an SMA element is analyzed showing the general characteristics of its dynamical response. Then, the analysis of an SMA-ATVA is carried out. This analysis starts by considering small amplitude vibrations in a way that the SMA element does not exhibit stress-induced phase transformation. Under this assumption, the SMA's influence is only due to stiffness changes. This kind of analysis is the most common in literature and is followed by an investigation concerning the influence of the hysteretic behavior due to stress-induced phase transformation by considering a proper description of the thermomechanical behavior of SMAs. All results from the SMA-ATVA are compared with those obtained from the classical TVA, establishing a proper contrast between the devices and their capacity to promote vibration reduction.

2. CONSTITUTIVE MODEL

The thermomechanical behavior of shape memory alloys may be modeled either by microscopic or macroscopic phenomenological points of view. Its description is the objective of numerous research efforts that try to contemplate all behavior details (Lagoudas, 2008; Paiva & Savi, 2006). Here, a constitutive model that is built upon the Fremond's model and previously presented by Paiva *et al.* (2005), Savi & Paiva (2005), Baêta-Neves *et al.* (2004) and Savi *et al.* (2002) is employed. This model considers different material properties for each phase and four macroscopic phases for the description of the SMA behavior. The tension–compression asymmetry, the plastic strain and the plastic-phase transformation coupling are incorporated in the original model. Nevertheless, for the sake of simplicity, these characteristics are not considered in this article. Therefore, the thermomechanical behavior of the SMA is described by the following set of equations:

$$\sigma = E\varepsilon + \left[E\alpha_h + \alpha\right](\beta_2 - \beta_1) - \Omega\,(T - T_0) \tag{1}$$

$$\dot{\beta}_1 = \frac{1}{\eta_1}\{\alpha\,\varepsilon + \Lambda_1(T) + (2\alpha\alpha_h + E\alpha_h^{\,2})(\beta_2 - \beta_1) + \alpha_h\left[E\varepsilon - \Omega\,(T - T_0)\right] - \partial_{\beta_1} J_\pi\} + \partial_{\dot{\beta}_1} J_\chi$$

$$\dot{\beta}_2 = \frac{1}{\eta_2}\{-\alpha\,\varepsilon + \Lambda_2(T) - (2\alpha\alpha_h + E\alpha_h^{\,2})(\beta_2 - \beta_1) - \alpha_h\left[E\varepsilon - \Omega\,(T - T_0)\right] - \partial_{\beta_2} J_\pi\} + \partial_{\dot{\beta}_2} J_\chi \tag{2}$$

$$\dot{\beta}_3 = \frac{1}{\eta_3}\left\{-\frac{1}{2}(E_A - E_M)\left[\varepsilon + \alpha_h(\beta_2 - \beta_1)\right]^2 + \Lambda_3(T) + (\Omega_A - \Omega_M)\,(T - T_0)\left[\varepsilon + \alpha_h(\beta_2 - \beta_1)\right] - \partial_{\beta_3} J_\pi\right\} + \partial_{\dot{\beta}_3} J_\chi$$

Here ε is the total strain, T is the temperature, β_1 and β_2 are the volume fractions of martensitic phases, respectively related to tension and compression, β_3 represents the volume fraction of austenite. Moreover, $E = E_M + \beta_3\,(E_A - E_M)$ is the elastic modulus while $\Omega = \Omega_M + \beta_3\,(\Omega_A - \Omega_M)$ is related to thermal expansion coefficient. Note that subscript A refers to austenitic phase, while M refers to martensite. Parameters $\Lambda_1 = \Lambda_2 = \Lambda = \Lambda(T)$ and $\Lambda_3 = \Lambda_3(T)$ are associated with phase transformation stress levels. Parameter α_h defines the horizontal width of the stress–strain hysteresis loop, while α controls the height of the same hysteresis loop. The terms $\partial_n J_\pi$ ($n = \beta_1, \beta_2, \beta_3$) are sub-differentials of the indicator function J_π with respect to n. This indicator function is related to a convex set π, which provides the internal constraints related to the phases' coexistence. With respect to evolution equations of volume fractions, $\eta_1 = \eta_2 = \eta$ and η_3 represent the internal dissipation related to phase transformations. Moreover $\partial_n J_\chi$ ($n = \beta_1, \beta_2, \beta_3$) are sub-differentials of the indicator function J_χ with respect to n. This indicator function is associated with the convex set χ, which establishes conditions for the correct description of internal sub-loops due to incomplete phase transformations. These sub-differentials may be replaced by Lagrange multipliers associated with the mentioned constraints (Savi *et al.*, 2002a).

Concerning parameter definitions, linear temperature dependent relations are adopted for Λ and Λ_3 as follows:

$$\Lambda = \begin{cases} -L_0 + \dfrac{L}{T_M}(T - T_M), & \text{if } T > T_M \\ -L_0, & \text{if } T \le T_M \end{cases} \quad ; \quad \Lambda_3 = \begin{cases} -L_0^A + \dfrac{L^A}{T_M}(T - T_M), & \text{if } T > T_M \\ -L_0^A, & \text{if } T \le T_M \end{cases} \tag{3}$$

Here T_M is the temperature below where the martensitic phase becomes stable. Usually, experimental tests provide information of M_s and M_f, temperatures where martensitic formation starts and finishes. This model uses only one temperature that could be an average value or alternatively, the M_f value. Moreover, L_0, L, L_0^A and L^A are parameters related to critical stress for phase transformation.

In order to describe the characteristics of phase transformation kinetics, different values of η and η_3 might be considered during loading, *i.e.* η^L and η_3^L, and unloading processes, *i.e.* η^U, η_3^U. For more details about the constitutive model see Paiva *et al.* (2005) and Savi & Paiva (2005). All constitutive parameters can be matched from stress-strain tests.

As it is well-known, SMA devices demonstrate the rate-dependence properties, i.e., their thermomechanical response depends on the rate of loading rate, see e.g., Shaw & Kyriakides (1995) and Yoon (2008). The adequate modeling of the rate-dependency of SMA's can be performed by considering the thermomechanical coupling terms in the energy equation. Monteiro Jr. *et al.* (2008) discussed the thermomechanical coupling in this constitutive model showing that it has rate-dependence characteristics even when these coupling terms are neglected. This viscous characteristic of the model allows one to capture the thermomechanical coupling avoiding the integration of the energy equation. Auricchio *et al.* (2006) explores the same idea showing the difference between a viscous model and a rate-independent model with thermomechanical coupling. Both models have the ability to describe pseudoelastic behavior in SMA wires. Hence, although martensitic transformations may be considered as non-diffusive for many practical applications, the model captures the rate-dependency from heat exchange which is useful for engineering purposes. Moreover, it is important to highlight that this rate dependency can be controlled by the proper choice of the model parameters.

3. SINGLE-DEGREE OF FREEDOM SHAPE MEMORY OSCILLATOR

Initially, the dynamical behavior of SMAs is analyzed by considering a single-degree of freedom oscillator (1DOF), which consists of a mass m attached to a shape memory element of length l and cross-sectional area A, and restitution force F_R. A linear viscous damper, associated with a parameter c, is also considered. Moreover, the system is harmonically excited by a force $F = F_0 \sin(\omega t)$. Figure 1 presents an oscillator where the restitution force, F_R, is provided by a general SMA element.

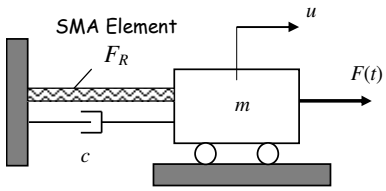

Figure 1: Single-degree of freedom oscillator.

The equation of motion of this oscillator may be formulated by considering the balance of linear momentum. The restitution force, $F_R = \sigma A$, may be provided by an SMA element described by the constitutive equations presented in the previous section (Paiva *et al.*, 2005). Therefore, the following equation of motion is obtained (Savi *et al.*, 2008):

$$m\ddot{u} + c\dot{u} + \frac{EA}{l}u + (A\alpha + EA\alpha_h)(\beta_2 - \beta_1) - \Omega A(T - T_0) = F_0 \sin(\omega t) \tag{4}$$

where volume fractions evolution β_1 and β_2 are described by the constitutive model presented in the preceding section. In order to obtain a dimensionless equation of motion, the system's parameters are defined as follows:

$$\delta = \frac{F_0}{ml\omega_0^2} = \frac{F_0}{E_R A};\quad \overline{\Omega} = \frac{\Omega_R A T_R}{ml\omega_0^2} = \frac{\Omega_R T_R}{E_R};\quad \overline{\alpha} = \frac{\alpha A}{ml\omega_0^2} = \frac{\alpha}{E_R};\quad \overline{\alpha}_h = \frac{\alpha_h E_R A}{ml\omega_0^2} = \alpha_h;$$
$$\omega_0^2 = \frac{E_R A}{ml};\quad \xi = \frac{c}{m\omega_0};\quad \mu_E = \frac{E}{E_R};\quad \mu_\Omega = \frac{\Omega}{\Omega_R};\quad \varpi = \frac{\omega}{\omega_0}. \tag{5}$$

Note that dimensionless parameters and variables are defined considering some reference values for temperature dependent parameters. This is done by assuming a reference temperature, T_R, where these parameters are evaluated. Parameters with subscript R are evaluated in this reference temperature. These definitions allow one to define the following dimensionless variables, respectively related to mass displacement (U), temperature (θ) and time (τ):

$$U = \frac{u}{l}; \quad \theta = \frac{T}{T_R}; \quad \tau = \omega_0 t \,. \tag{6}$$

Therefore, the dimensionless equation of motion has the form:

$$U'' + \xi U' + \mu_E U + (\overline{\alpha} + \mu_E \overline{\alpha}_h)(\beta_2 - \beta_1) - \mu_\Omega \overline{\Omega}(\theta - \theta_0) = \delta \sin(\varpi \tau) \tag{7}$$

where derivatives with respect to dimensionless time are represented by $(\,)' = d(\,)/d\tau$. Besides the nonlinear SMA oscillator, an elastic single-degree of freedom oscillator is analyzed by replacing the SMA element by an elastic element where the restitution force is given by $F_R = ku$ and its natural frequency is $\omega_L = \sqrt{k/m}$. The equivalent elastic oscillator is governed by:

$$U'' + \xi U' + \frac{\omega_L^2}{\omega_0^2} U = \delta \sin(\varpi \tau) \tag{8}$$

3.1. Numerical Simulation

In order to deal with nonlinearities of the SMA oscillator equations of motion, an iterative procedure based on the operator split technique (Ortiz *et al.*, 1983) is employed. Under this assumption, the fourth-order Runge–Kutta method is used together with the projection algorithm proposed by Savi *et al.* (2002) to solve the constitutive equations. The solution of the constitutive equations also employs the operator split technique together with an implicit Euler method. The calculation of β_n (n = 1,2,3) considers that the evolution equations are solved in a decoupled way. At first, the equations (except for the sub-differentials) are solved using an iterative implicit Euler method. If the estimated results obtained for β_n do not satisfy the imposed constraints, an orthogonal projection algorithm pulls their value to the nearest point on the domain's surface (Paiva *et al.*, 2005a). On the other hand, the numerical integration of the linear system uses the classical Runge-Kutta approach.

For the numerical investigation it is considered a linear system with m = 1 and ω_L=0.72ω_0. In the case of the SMA oscillator, the same single-degree of freedom oscillatory system is considered, however, the linear elastic element is replaced by an SMA element. The SMA parameters used in numerical simulations are presented in Table 1. At this point, all simulations are carried out with T = 372K, a high temperature where austenite is stable for a stress-free state. Moreover, it is considered an SMA element with A=1.96×10^{-5}m and l=50×10^{-3}m.

Table 1: SMA parameters

E_A (GPa)	E_M (GPa)	α (MPa)	α_h	L_0 (MPa)	L (MPa)	L_0^A (MPa)	L^A (MPa)
54	42	330	0.048	0.15	41.5	0.63	185
Ω_A (MPa/K)	Ω_M (MPa/K)	T_M (K)	η^L (MPa.s)	η^U (MPa.s)	η_3^L (MPa.s)	η_3^U (MPa.s)	
0.74	0.17	291.4	1.0	2.7	1.0	2.7	

The numerical simulations starts by considering the undamped oscillators with ω=0.72ω_0 and δ=0.01. Under these conditions, the linear system presents the well-known resonant response showed in Figure 2(a). The SMA oscillator response, however, tends to attenuate the amplitude response, as showed in Figure2(b), due to the hysteretic behavior of the SMA element. Figure 2(c) presents the correspondent stress-strain curve of the SMA oscillator.

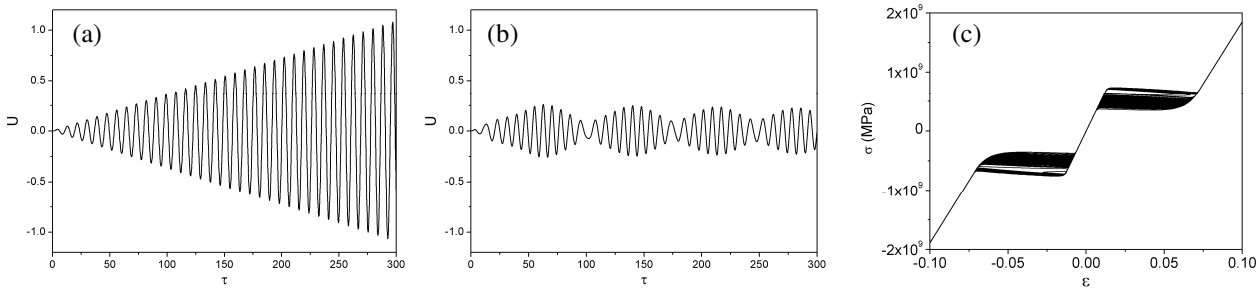

Figure 2: Undamped system response for ω=0.72ω_0: (a) Linear oscillator; (b) SMA oscillator. (c) Stress-strain curve related to the SMA system.

Considering now the damped situation (ξ=0.05) for both oscillators, the linear system response tends to stabilize in a specific amplitude, as showed in Figure 3(a). Once again the hysteretic behavior of the SMA oscillator tends to attenuate the amplitude response when compared to the linear system, as showed in Figure 3(b). Figure 3(c) presents the correspondent stress-strain curve of the SMA oscillator.

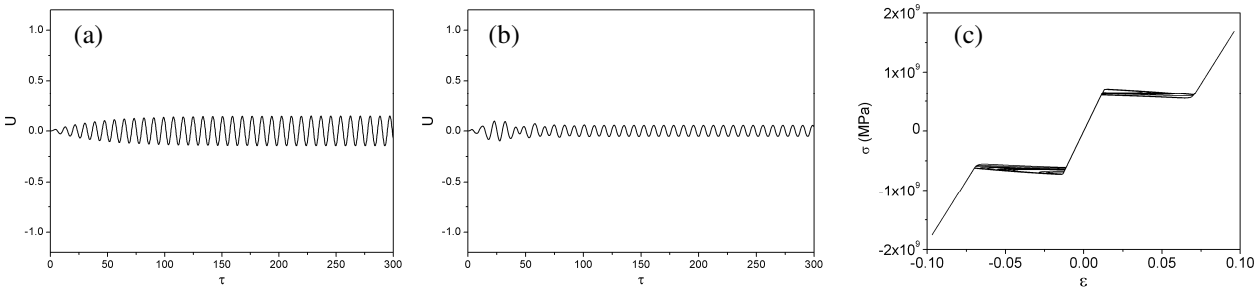

Figure 3: Damped (ξ=0.05) system response for ω=0.72ω_0: (a) Linear oscillator; (b) SMA oscillator. (c) Stress-strain curve related to the SMA system

Due to nonlinearities, the SMA oscillator response is far more complex than the linear oscillator response. In order to identify the resonant characteristics of the SMA oscillator, nonlinear resonant curves are plotted by increasing and decreasing forcing frequency. In both situations, the system is numerically integrated assessing the maximum steady state amplitude, as showed in Figure 4 for δ=0.008 and δ=0.012. It is evident that nonlinearities introduce dynamical jumps to the system response and that the variation in forcing amplitude changes the frequency where jumps occur. Moreover, it should be highlighted that the response of the SMA system tends to present smaller vibration amplitude when compared to those obtained by the elastic oscillator. This result shows some aspects of the SMA's dynamical response. The next section addresses the use of SMA elements in secondary system used in vibration absorbers.

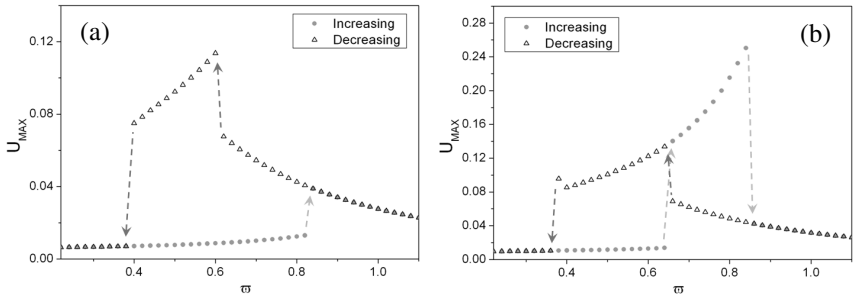

Figure 4: Maximum amplitudes response for increased and decreased forcing frequency. (a) δ=0.008; (b) δ=0.012.

4. NONLINEAR VIBRATION ABSORBERS

The tuned vibration absorber (TVA) is a well-established vibration control device, which can be used to attenuate the vibration of a primary system at a particular forcing frequency. The goal of the passive vibration absorber is to dissipate energy of the primary system, reducing its vibration amplitudes in a specific forcing frequency. This goal is achieved by choosing the absorber natural frequency equal to the forcing frequency in which the vibration reduction is needed (Inman, 1989; Meirovitch, 1986).

The adaptive TVA (ATVA) is an adaptive–passive vibration control device similar to a TVA but with adaptive elements that can be used to change the ATVA tuned condition. The aim of ATVAs with SMA elements is to attenuate primary system vibration amplitudes, not only for one specific forcing frequency, as occurs with the TVA, but for a range of frequencies exploring the temperature dependent characteristic of the SMAs. This section investigates the SMA-ATVA dynamics by establishing a comparison between two different absorbers: a TVA and an SMA-ATVA. The analysis of the SMA-ATVA is done by considering two different approaches. The first investigates small amplitude response that does not induce stress-induced phase transformation, which is the classical approach in literature. On the other hand, the second approach considers stress-induced phase transformations and therefore, is associated with energy dissipation due to hysteretic behavior.

Figure 5 presents a two-degree of freedom system that represents a primary system, subsystem (m_1, c_1, k_1), that is harmonically excited by an external force $F = F_0\sin(\omega t)$ and which vibration amplitudes wish to be reduced by using a secondary system that consists of a concentrated mass, m_2, attached viscous damping, c_2, and to an element with restoring force F_R. This element could be an SMA element with length l and transversal section area A, defining an SMA-ATVA system or a linear element defining a classical TVA.

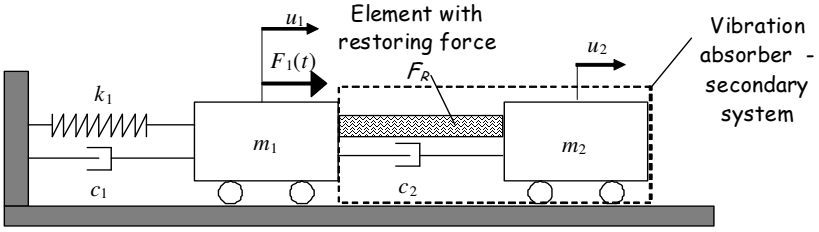

Figure 5: Vibration absorber connected to a primary system.

Both classical TVA and the SMA-ATVA systems may be described by the following equations of motion:

$$\begin{cases} m_1\ddot{u}_1 + (c_1 + c_2)\dot{u}_1 - c_2\dot{u}_2 + k\,u_1 - F_R = F_0\sin(\omega t) \\ m_2\ddot{u}_2 - c_2\dot{u}_1 + c_2\dot{u}_2 + F_R = 0 \end{cases} \tag{9}$$

The description of the restitution force depends on the kind of absorber. The SMA-ATVA has a restitution force F_R that is described by the constitutive equation presented in section 2. Therefore, the SMA-ATVA system has the following equations of motion together with the SMA constitutive equation:

$$\begin{cases} m_1\ddot{u}_1 + (c_1 + c_2)\dot{u}_1 - c_2\dot{u}_2 + k\,u_1 - \dfrac{EA}{l}(u_2 - u_1) - (A\alpha \ + EA\alpha_h)(\beta_2 - \beta_1) + \\ \quad + \Omega A(T - T_0) = F_0\sin(\omega t) \\ m_2\ddot{u}_2 - c_2\dot{u}_1 + c_2\dot{u}_2 + \dfrac{EA}{l}(u_2 - u_1) + (A\alpha \ + EA\alpha_h)(\beta_2 - \beta_1) - \Omega A(T - T_0) = 0 \end{cases} \tag{10}$$

In order to obtain a dimensionless equation of motion, system's parameters are defined as follows:

$$\omega_{01}^2 = \frac{k}{m_1}\ ;\quad \omega_{02}^2 = \frac{E_R A}{m_2 l}\ ;\ \xi_1 = \frac{c_1}{m_1\omega_{02}}\ ;\ \xi_2 = \frac{c_2}{m_2\omega_{02}}\ ;\ \gamma_\omega = \frac{\omega_{01}^2}{\omega_{02}^2}\ ;\ \gamma_m = \frac{m_2}{m_1}\ ;\ \overline{\alpha}\ = \frac{\alpha\ A}{m_2 l\omega_{02}^2} = \frac{\alpha}{E_R}\ ;$$

$$\overline{\alpha}_h = \frac{\alpha_h E_R A}{m_2 l\omega_{02}^2} = \alpha_h\ ;\ \delta = \frac{F_0}{m_1 l\omega_{02}^2} = \frac{m_2}{m_1}\frac{F_0}{E_R A}\ ;\ \overline{\Omega} = \frac{\Omega_R A T_R}{m_2 l\omega_{02}^2} = \frac{\Omega_R T_R}{E_R}\ ;\ \mu_E = \frac{E}{E_R}\ ;\ \mu_\Omega = \frac{\Omega}{\Omega_R}\ ;\ \varpi = \frac{\omega}{\omega_{02}} \tag{11}$$

These definitions allow one to define the following dimensionless variables, respectively related to mass displacements (U_1,U_2), temperature (θ) and time (τ):

$$U_1 = \frac{u_1}{l}\ ;\ U_2 = \frac{u_2}{l}\ ;\quad \theta = \frac{T}{T_R}\ ;\quad \tau = \omega_{02}t\ . \tag{12}$$

Moreover, the TVA has a linear restitution force, $F_R = k_L(u_2 - u_1)$, that results in the following dynamical system:

$$U_1'' + \left(\xi_1 + \frac{m_2}{m_1}\xi_2\right)U_1' - \frac{m_2}{m_1}\xi_2 U_2' + \left(\frac{\omega_{L1}^2}{\omega_{02}^2} + \frac{m_2}{m_1}\frac{\omega_{L2}^2}{\omega_{02}^2}\right)U_1 - \frac{m_2}{m_1}\frac{\omega_{L2}^2}{\omega_{02}^2}U_2 = \delta\sin(\varpi\tau)$$

$$U_2'' - \xi_2 U_1' + \xi_2 U_2' - \frac{\omega_{L2}^2}{\omega_{02}^2}U_1 + \frac{\omega_{L2}^2}{\omega_{02}^2}U_2 = 0 \tag{13}$$

where $\omega_{L1}^2 = \dfrac{k_1}{m_1}$ and $\omega_{L2}^2 = \dfrac{k_L}{m_2}$.

This article considers a primary system with m_1=5kg and $k_1 = 5k_L$. It is assumed a critical case where the primary system is under resonant conditions. Initially, the TVA is of concern and the mass and the stiffness values are chosen in such a way that the natural frequency of the primary system is the same as the single-degree of freedom oscillator considered in the last section: m_2=1kg and $k_L = 0.72^2 \times E_R A/l$. Figure 6 presents the response of the TVA primary system showing the maximum amplitudes as a function of the forcing frequency with δ=0.01. Two different damping coefficients are analyzed representing an undamped system (ξ_1=ξ_2=0) and a damped system (ξ_1=ξ_2=0.2). These results

are compared with the single-degree of freedom oscillator response. It can be observed that for $\varpi = 0.72$, critical resonant situation for the 1DOF oscillator, the absorber reduces the amplitude of the primary system response. Nevertheless, the new degree of freedom related to the secondary system introduces two resonant frequencies, identified in $\omega_1 = 0.58\varpi$ and $\omega_2 = 0.9\varpi$. The undamped system presents amplitudes that increase indefinitely in these frequencies while the damping tends to limit the amplitude increase as shown in Figure 6.

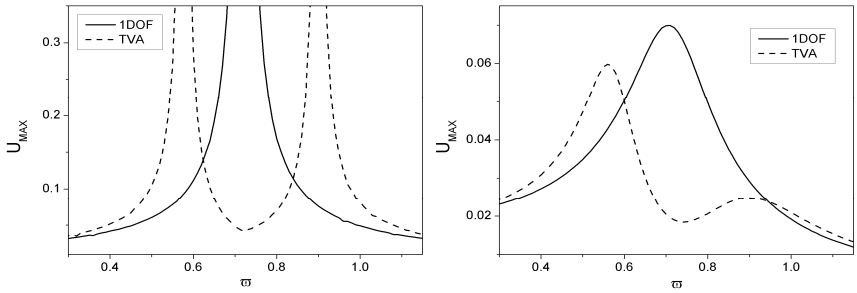

Figure 6: Maximum amplitudes response of the 1DOF linear oscillator and of the TVA primary system with δ=0.01. Left: ξ_1=ξ_2=0; Right: ξ_1=ξ_2=0.2.

The forthcoming analysis discusses the ATVA with an SMA element, showing how it can be useful for vibration reduction. Two different analyses are developed by exploring the hysteresis loop related to stress-induced phase transformations or the absence thereof. Initially, small amplitude movement is of concern and, therefore, the SMA element does not present stress-induced phase transformations. These phase transformations can also be avoided by using steel beam elements in parallel with SMA elements as have been observed by Williams *et al.* (2005). Under this condition, it is possible to alter the absorber natural frequencies due to the change of the element's stiffness caused by temperature-induced phase transformations. In this regard, two different ranges of temperatures are considered: temperatures where martensite is stable (below T_M), and temperatures where austenite is stable (higher than T_A = 307.5K). The same characteristics of the primary oscillator (m_1=5kg, $k = 5\times0.72^2\times E_R A/l$) are assumed and the vibration absorber has an SMA element with the same characteristics discussed in the previous section (m_2=1kg, $A = 1.96\times10^{-5} m^2$ and $l = 50\times10^{-3} m$). Figure 7 presents a comparison between system responses for two different temperatures, showing that it is possible to change the range of frequencies where the primary system amplitude reduction is achieved by changing the temperature. This kind of behavior increases the frequency range where the ATVA can be efficiently used, which is an essential advantage when compared to the elastic TVA.

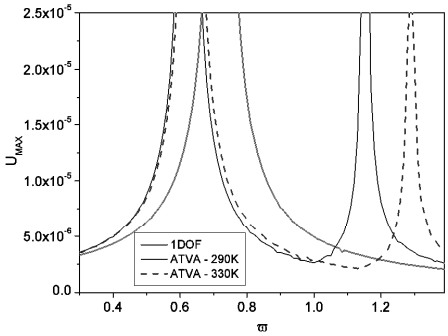

Figure 7: SMA-ATVA primary system maximum amplitudes response for different temperatures.

Although temperature-induced phase transformations can provide flexibility to the SMA-ATVA response, when compared to the classical TVA, the system response may be better explored by assuming large amplitudes of the SMA element that causes stress-induced phase transformations related to hysteretic behavior. The following analysis explores both temperature-induced phase transformation variation and hysteretic behavior due to stress-induced phase transformations as well.

4.1. SMA-ATVA Exploring Stress-induced Hysteresis Loop

At this point, we consider the general application of the SMA-ATVA where the amplitudes are no longer limited to small oscillations. Under this new condition, stress-induced phase transformations occur corresponding with the hysteresis loop. This behavior is related to strong nonlinearities that are usually associated with complex responses. The analysis is focused on the influence of temperature on the system response, but considering just high temperatures,

which means that the SMA element is initially at austenitic phase. Figures 8(a)-9(a) shows the SMA element stress-strain curve at 340K and 540K, showing typical pseudoelastic behavior confirming this argument. Note that the increase in temperature causes the increase of the critical stress level where phase transformation begins to occur. Therefore, we can understand that the increase in temperature is related to the higher position of the hysteresis loop in the stress-strain space, and this behavior is useful for vibration reduction purposes.

The system response is now analyzed in order to verify the influence of temperature variation on vibration reduction. The previous temperatures are of concern (340K and 540K). Figure 8 presents: (b) the displacement time history of the primary system and (c) the stress-strain curve of the SMA element. Parameters $\varpi = 0.58$, δ=0.0075, ξ_1=ξ_2=0.1 are assumed at T=540K. Under these conditions, the SMA element does not present phase transformation and, therefore, the amplitudes is not enough to pass through the hysteresis loop. This kind of behavior makes this response similar to the elastic TVA. Decreasing the temperature to T=340K, the hysteresis loop tends to be in a lower position on the stress-strain space as shown in Figures 8(a)-9(a). Therefore, the dynamical response of the system starts to dissipate energy due to the hysteresis loop and this large amount of energy dissipation tends to reduce the vibration amplitudes of the primary system. Figure 9(b-c) presents the system response represented by the displacement time history of the primary system and the stress-strain curve of the SMA element, confirming the expected behavior.

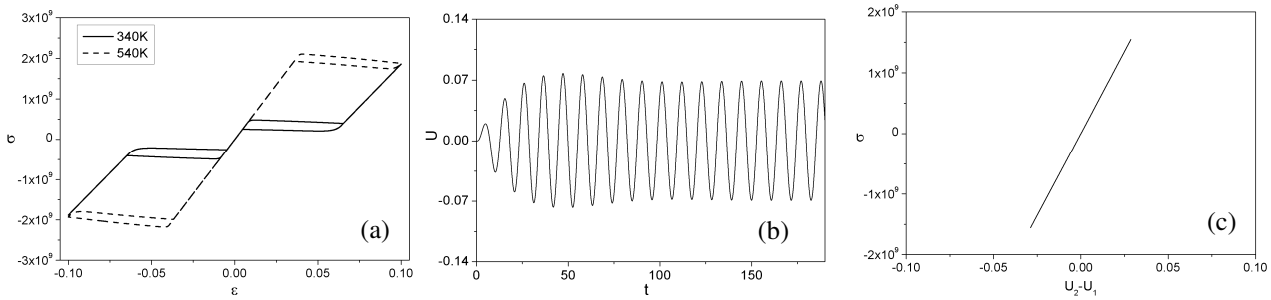

Figure 8: (a) Stress-strain curve; (b-c) Primary system time response and stress-strain curve at T=540K.

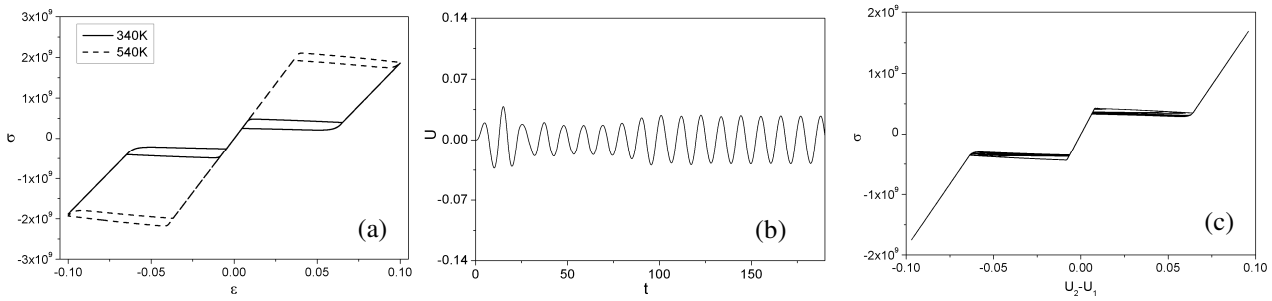

Figure 9: (a) Stress-strain curve; (b-c) Primary system time response and stress-strain curve at T=340K.

Although we can achieve a more efficient vibration reduction due to hysteretic energy dissipation, dynamical jumps can make the system response different. A more detailed analysis of the system should be considered for a proper design of the absorber. Figure 10 establishes a comparison among the displacement time history of the primary system considering three different conditions: TVA, ATVA at T=540K and ATVA at T=340K. Two different frequencies are of concern showing how it can change primary system vibration absorption.

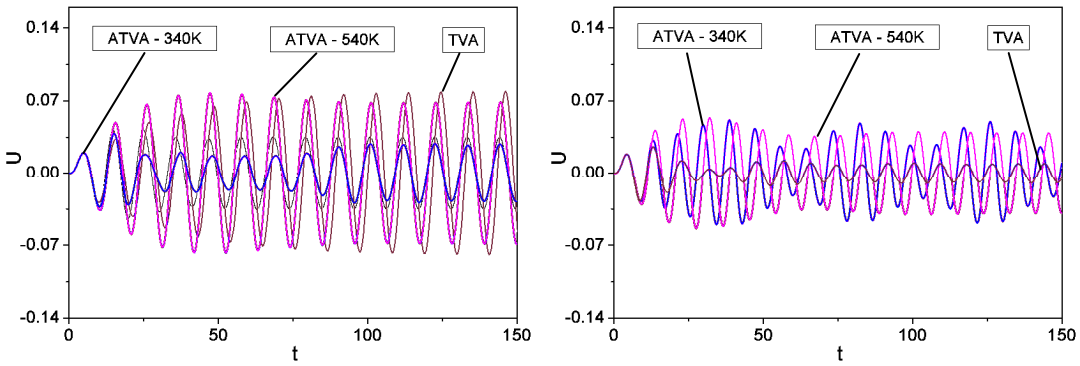

Figure 10: TVA and ATVA primary system time responses.
Left: ϖ=0.58; Right: ϖ=0.72.

The previous results can be better understood by considering the frequency domain response expressed in terms of the maximum amplitudes as a function of forcing frequency. Figure 11 presents this frequency domain response for the same results showed in Figures 8-10. It can be observed that the better performance of each absorber depends on temperature and excitation conditions. For some forcing frequencies it is noticed that the ATVA tends to present better performance, however, for different forcing frequencies the TVA can achieve smaller primary system amplitudes responses. Moreover, the ATVA at T=340K presents smaller amplitudes responses for forcing frequencies around ϖ =0.6 when compared to its performance at T=540K. This kind of behavior is due to the energy dissipation associated with hysteresis loop, which does not happen at the higher temperature. It should be highlighted that differences from the elastic TVA and the SMA-ATVA performances could be altered by temperature variations.

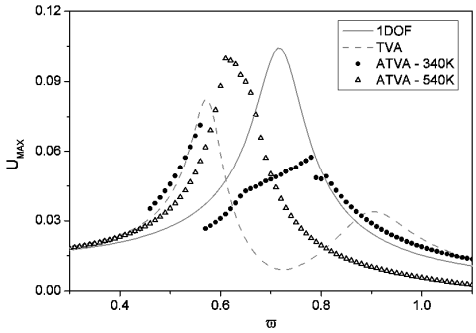

Figure 11: TVA and ATVA primary system maximum amplitudes response for δ=0.0075 and $\xi_1=\xi_2$=0.1.

5. CONCLUSIONS

This article discusses the use of SMA elements in vibration absorbers. The thermomechanical behavior of SMAs is described by the constitutive model proposed by Paiva *et al.* (2005). Initially, a single-degree of freedom oscillator is presented in which the restitution force is given by the SMA element. The analysis of this system shows that the hysteretic behavior is related to high energy dissipation, indicating the use of SMA element in a vibration absorber. The next step of this work consists in the dynamical analysis of an adaptive absorber composed of a SMA element (ATVA). The behavior of this system is then compared with a passive absorber, composed of a linear element (TVA). The TVA attenuates the primary system vibration amplitudes in a chosen forcing frequency, however, two new resonance frequencies appear and must be avoided. The SMA-ATVA is capable of reducing the system response amplitudes not only in the initially chosen forcing frequency but also in these two new resonant frequencies that appear in the TVA. This happens as a consequence of the energy dissipation associated with the mechanical properties variation due to temperature-induced phase transformations and also related to the hysteretic behavior due to stress-induced phase transformation. SMA actuators have a great potential to be used in vibration control, nevertheless, it is important to mention that the strong nonlinear behavior of SMAs may introduce unusual, complex dynamical responses that should be further investigated during the design of the application. The parametric analysis developed in this paper shows different kinds of possibilities related to the response of SMA absorbers.

6. ACKNOWLEDGEMENTS

The authors would like to acknowledge the support of the Brazilian Research Agency (CNPq), the State Research Agency (FAPERJ) and ELETRONORTE. The Air Force Office of Scientific Research (AFOSR) is also acknowledged and it is important to mention the inspirational discussions with James M. Fillerup and Victor Giurgiutiu.

7. REFERENCES

Auricchio, F., Fugazza, D. & DesRoches, R. (2006), "Numerical and experimental evaluation of the damping properties of shape-memory alloys", *Journal of Engineering Materials and Technology - ASME*, v.128, pp.312-319.

Baêta-Neves, A.P., Savi, M.A. & Pacheco, P.M.C.L. (2004), "On the Fremond's constitutive model for shape memory alloys", *Mechanics Research Communications*, v.31, n.6, pp.677-688.

Bernardini, D. & Rega, G. (2005), "Thermomechanical modelling, nonlinear dynamics and chaos in shape memory oscillators", *Mathematical and Computer Modelling of Dynamical Systems*, v.11, n.3, pp.291-314.

Brennan, M.J. (2006), "Some recent developments in adaptive tuned vibration absorbers/neutralisers", *Shock and Vibration* , v.13, n.4-5, pp.531-543.

Elahinia, M.H., Koo, J.H. & Tan, H. (2005), "Improving robustness of tuned vibration absorbers using shape memory alloys", *Shock and Vibration*, v.12, n.5, pp.349-361.

Ibrahim, R.A. (2008), "Recent advances in nonlinear passive vibration isolators", *Journal of Sound and Vibration*, v.314, n.3-5, pp.371-452.

Inman, D.J. (1989), "*Vibration with Control, Measurement and Stability*", Prentice Hall.

Lagoudas, D.C. (2008), "*Shape Memory Alloys: Modeling and Engineering Applications*", Springer.

Lagoudas, D.C., Khan, M.M., Mayes, J.J. & Henderson, B.K. (2004), "Pseudoelastic SMA spring elements for passive vibration isolation: Part II - Simulations and experimental correlations", *Journal of Intelligent Material Systems and Structures*, v.15, n.6, pp.443-470.

Machado, L.G. & Savi, M.A. (2003), "Medical applications of shape memory alloys", *Brazilian Journal of Medical and Biological Research*, v.36, n.6, pp.683-691.

Machado, L.G., Savi, M.A. & Pacheco, P.M.C.L. (2003), "Nonlinear dynamics and chaos in coupled shape memory oscillators", *International Journal of Solids and Structures*, v.40, n.19, pp.5139-5156.

Machado, L.G., Lagoudas, D.C. & Savi, M.A. (2009), "Lyapunov exponents estimation for hysteretic systems", *International Journal of Solids and Structures*, v.46, n.6, pp.1269-1598.

Meirovitch, L. (1986), "*Elements of Vibration Analysis*", McGraw-Hill.

Monteiro Jr, P.C.C., Savi, M.A., Netto, T.A. & Pacheco, P.M.C.L. (2008), "A phenomenological description of the thermomechanical coupling and the rate-dependent behavior of shape memory alloys", submitted to the *Journal of Intelligent Material Systems and Structures*.

Ortiz, M., Pinsky, P.M. & Taylor, R.L. (1983), "Operator split methods for the numerical solution of the elastoplastic dynamic problem", *Computer Methods of Applied Mechanics and Engineering*, v. 39, pp.137-157.

Paiva, A., Savi, M.A., Braga, A.M.B. & Pacheco, P.M.C.L. (2005), "A constitutive model for shape memory alloys considering tensile-compressive asymmetry and plasticity", *International Journal of Solids and Structures*, v.42, n.11-12, pp.3439-3457.

Paiva, A. & Savi, M.A. (2006), "An overview of constitutive models for shape memory alloys", *Mathematical Problems in Engineering*, 2006, v.2006, Article ID56876, pp.1-30.

Rustighi, E., Brennan, M. J. & Mace, B. R. (2005a), "A shape memory alloy adaptive tuned vibration absorber: design and implementation", *Smart Material and Structures*, v.14 pp.19–28.

Rustighi, E., Brennan, M. J. & Mace, B. R. (2005b), "Real-time control of a shape memory alloy adaptive tuned vibration absorber", *Smart Material and Structures*, v.14 pp.1184–1195.

Saadat, S., Salichs, J., Noori, M., Hou, Z. Davoodi, H., Bar-On, I., Suzuki, Y. & Masuda, A. (2002), "An overview of vibration and seismic applications of NiTi shape memory alloy", *Smart Materials and Structures*, v.11, n.2, pp.218-229.

Salichs, J., Hou, Z. & Noori, M. (2001), "Vibration suppression of structures using passive shape memory alloy energy dissipation devices", *Journal of Intelligent Material Systems and Structures*, v.12, n.10, pp.671-680.

Santos, B.C. & Savi, M.A. (2007), "Nonlinear dynamics of a nonsmooth shape memory alloy oscillator", *Chaos, Solitons and Fractals*. doi:10.1016/j.chaos.2007.07.058.

Savi, M. A. & Pacheco, P. M. L. C. (2002), "Chaos and hyperchaos in shape memory systems", *International Journal of Bifurcation and Chaos*, v.12, n.3, pp.645-657.

Savi, M.A., Paiva, A., Baêta Neves, A.P. & Pacheco, P.M.C.L. (2002), "Phenomenological modeling and numerical simulation of shape memory alloys: A thermo-plastic-phase transformation coupled model", *Journal of Intelligent Material Systems and Structures*, v.13, n.5, pp.261-273.

Savi, M.A. & Paiva, A. (2005), "Describing internal subloops due to incomplete phase transformations in shape memory alloys", *Archive of Applied Mechanics*, v.74, n.9, pp.637-647.

Savi, M.A., Sa, M.A.N., Paiva, A. & Pacheco, P.M.C.L. (2008), "Tensile-compressive asymmetry influence on the shape memory alloy system dynamics", *Chaos, Solitons and Fractals*, v.36, pp.828-842.

Shaw, J. A. & Kyriades, S. (1995), "Thermomechanical aspects of Ni-Ti", *Journal of the Mechanics and Physics of Solids*, v.43, n.8, pp.1243-1281.

Sitnikova, E., Pavlovskaia, E. Wiercigroch, M. & Savi, M.A. (2008), "Vibration reduction of the impact system by an SMA restraint: Numerical studies", submitted to *International Journal of Non-linear Mechanics*.

Sitnikova, E., Pavlovskaia, E. & Wiercigroch, M. (2008), "Dynamics of an impact oscillator with SMA constraint", *European Physical Journal - Special Topics*, v.165, pp.229-238.

van Humbeeck, J. (2003), "Damping capacity of thermoelastic martensite in shape memory alloys", *Journal of Alloys and Compounds*, v.355, pp.58–64.

Williams, K., Chiu, G. & Bernhard, R. (2002), "Adaptive-passive absorvers using shape-memory alloys", *Journal of Sound and Vibration*, v.249, n.5, pp.835-848.

Williams, K., Chiu, G. & Bernhard, R. (2005), "Dynamic modelling of a shape memory alloy adaptive tuned vibration absorber", *Journal of Sound and Vibration*, v.280, pp.211-234.

Yoon, S.H. (2008), "Experimental investigation of thermo-mechanical behaviors in Ni-Ti shape memory alloy", *Journal of Intelligent Material Systems and Structures*, v.19, n.3, pp.283-289.